JOURNAL OF COMPUTATIONAL PHYSICS 96, 99–109 (1991)

# Preconditioned Descent Algorithm for Rapid Calculations of Magnetohydrodynamic Equilibria*

S. P. HIRSHMAN

*Oak Ridge National Laboratory, Oak Ridge, Tennessee 37831*

AND

O. BETANCOURT

*City College, CUNY, New York, New York 10038*

Received October 6, 1989; revised April 6, 1990

Conjugate gradient descent algorithms have been used in several magnetohydrodynamic (MHD) equilibrium codes to find numerical minima of the MHD energy and thus to locate local stable equilibria. Numerical convergence studies with the spectral equilibrium code VMEC (variational moments equilibrium code) have shown that the number of descent iterations required to obtain a fixed level of convergence grows linearly with the number of radial mesh points. This undesirable mesh dependence is due to the quadratic dependence on the radial mesh spacing of the condition number for the linearized discrete MHD equations. By use of a preconditioning matrix to coalesce the eigenvalues of the linearized MHD forces around unity, it is possible to reduce the condition number substantially and thereby nearly eliminate the mesh size dependence of the convergence rate of the descent algorithm. An invertible, positive-definite tridiagonal preconditioning matrix is derived from the force equations used in VMEC, and the improvement in temporal convergence is demonstrated for several three-dimensional equilibria.

## 1. INTRODUCTION

Improvements in the accuracy [1] and speed [2] of numerical computations of magnetohydrodynamic (MHD) equilibria based on energy minimization have recently been reported. In this paper, the preconditioning algorithm described in Ref. [2] has been adapted to the spectral equilibrium code VMEC [1]. The result is to essentially eliminate any dependence of the convergence rate on the number of radial grid points, $N_s$. The resultant preconditioned code is capable of analyzing

* Research sponsored by the Office of Fusion Energy, U.S. Department of Energy, under Contract DE-AC05-84OR21400 with Martin Marietta Energy Systems, Inc., and under Contract DE-FG02-86ER-53223 with City College of the City University of New York.

equilibria on very fine radial meshes ($N_s \sim 10^2$). It can therefore be used in stability calculations where extremely accurate equilibria are required to analyze radially localized modes [3].

The equilibrium code VMEC solves the MHD force balance equation $\mathbf{F}_{\mathrm{MHD}} \equiv \mathbf{J} \times \mathbf{B} - \nabla p = 0$ in three-dimensional (3D) toroidal geometry. Here, $\mathbf{J} = \mu_0 \nabla \times \mathbf{B}$ is the plasma current, $\mathbf{B}$ is the magnetic field, and $p$ is the isotropic plasma pressure. Fourier analysis is performed in the two angular coordinates $(\theta, \phi)$, and a grid is used for the remaining dependence on the radial coordinate, $s$. Extensive numerical convergence studies with VMEC have shown that the number of iterations required for convergence of the force residual $|\mathbf{F}_{\mathrm{MHD}}|^2$ grows linearly with the number of radial grid points. This unfavorable scaling with $N_s$ is due to the second-order spatial derivative structure of the MHD force operator, which implies a condition number $P \sim N_s^2$. (The condition number for the nonlinear MHD equilibrium problem is defined as the ratio of the largest to the smallest eigenvalue of the linearized MHD force operator at a fixed time.) A second-order temporal integration scheme is used in VMEC (see Eq. (2a)), so that the convergence time scales as $P^{1/2} \sim N_s$.

Clearly, a reduction in $P$ will improve the convergence rate of any descent algorithm based on an energy minimizing principle. In the MHD problem of interest here, the energy functional is $W = \int (B^2/2\mu_0 + p/(\gamma - 1))\, dV$. ($\gamma$ is the adiabatic index, which is chosen to be $\frac{5}{3}$ in the present calculations.) A well-known technique for reducing $P$ is to "precondition" the energy gradient vector $(-\nabla W)$ by a positive matrix $\mathbf{M}$ so that $-\mathbf{M} \cdot \nabla W$ is approximately diagonal, with the diagonal elements nearly equal to one [4]. In Section 2, such a preconditioning matrix is derived for the set of spectral equilibrium equations used in VMEC. Then, in Section 3, the mesh dependence of the convergence rate for the temporal iteration scheme based on the preconditioned forces is contrasted with that of the one based on the original (unconditioned) MHD forces.

## 2. Derivation of Preconditioning Matrix for the MHD Inverse Equilibrium Equations

The VMEC code obtains the solution of the MHD energy minimization problem by solving for the cylindrical coordinates $(R, \phi, Z)$ in terms of the toroidal flux (radial) coordinate $s$, toroidal angle $\zeta$, and poloidal angle $\theta$. The equations are simplified by choosing the toroidal angle $\zeta = \phi$. Let $x_1 \equiv R$ and $x_2 \equiv Z$. In VMEC, these coordinates are expanded in Fourier series:

$$x_\alpha = \sum_{m=0}^{M} \sum_{n=-N}^{N} \sum_{j=1}^{N_s} X_\alpha^{mn}(s_j) \exp[i(m\theta - n\phi)]. \tag{1}$$

In Eq. (1), $s_j$ denotes the equally spaced radial (flux) nodes for $j = 1, \ldots, N_s$ and $X_\alpha^{mn}$ are the Fourier amplitudes of $x_\alpha$ (for $\alpha = 1, 2$) which are to be determined by the

energy minimization. Variation of the discretized MHD energy $W = \int (B^2/2\mu_0 + p/(\gamma - 1))\, dV$ yields gradients, $F_\alpha^{mn} \equiv -\partial W/\partial X_\alpha^{mn}$, which must vanish in the equilibrium state: $F_\alpha^{mn} = 0$. Here, $F_\alpha^{mn}$ are the transforms of the cylindrical $(\nabla x_\alpha)$ components of the MHD force $\mathbf{F}_{\mathrm{MHD}} = \mathbf{J} \times \mathbf{B} - \nabla p$.

The expressions for $F_\alpha^{mn}$ are nonlinear functions [5] of $\mathbf{X}$, as well as the spatial derivatives $d\mathbf{X}/ds$ and $d^2\mathbf{X}/ds^2$. Here, $\mathbf{X} = \{X_1^{0,-N}, ..., X_1^{MN}, X_2^{0,-N}, ..., X_2^{MN}\}$ denotes the vector of Fourier amplitudes of $R$ and $Z$. Because of this nonlinearity, and the typically large number of harmonics needed to accurately describe realistic equilibria, an iterative scheme has been developed to solve the simultaneous coupled nonlinear equations $F_\alpha^{mn}(\mathbf{X}) = 0$ for the coordinate transform amplitudes $X_\alpha^{mn}(s_j)$. A second-order Richardson scheme [3] is used to evolve $\mathbf{X}$ to the equilibrium state $F_\alpha^{mn}(\mathbf{X}) = 0$:

$$L_t(X_\alpha^{mn}) \equiv \frac{d^2 X_\alpha^{mn}}{dt^2} + \frac{1}{\tau}\frac{dX_\alpha^{mn}}{dt} = F_\alpha^{mn}(\mathbf{X}). \tag{2a}$$

Multiplying Eq. (2a) by $dX_\alpha^{mn}/dt$ and summing over modes and mesh points leads to the energy dissipation relation

$$\frac{d(W_K + W)}{dt} = -\frac{1}{\tau} W_K, \tag{2b}$$

where $W_K = \frac{1}{2}\sum_{j,m,n,\alpha} [dX_\alpha^{mn}(s_j)/dt]^2 \geq 0$ is the "kinetic" energy. Equation (2b) guarantees the descent of the MHD energy, $W$, to a local minimum value.

Equation (2a) forms the basis of a temporal iteration scheme for obtaining the Fourier amplitudes $\mathbf{X}$ in the equilibrium state. As shown in Appendix A, Eq. (2a) may be integrated over the time interval $t \in [t_n, t_{n+1} = t_n + \Delta t]$ to yield a second-order, explicit iteration method which is a generalization to nonlinear systems of the standard (linear) conjugate gradients algorithm [6].

The number of iterations required for convergence of the iterative scheme in Eq. (A2) can be estimated by linearizing the force in Eq. (2a) around an equilibrium solution, $\mathbf{X} = \mathbf{X}_{\mathrm{EQ}}$. Let $f_\alpha(x_\alpha, s, \theta, \phi)$ denote the real-space representation of the MHD force components (i.e., the inverse transform of $F_\alpha^{mn}(\mathbf{X})$). The spatial discretization of the second-order partial differential operator $f_\alpha$ yields a matrix with a condition number $P$ proportional to the sum of the squares of the number of mesh points (or Fourier modes) in each coordinate direction. If the iteration is interpreted as a discretized "artificial" time operator [7], then the steady-state (equilibrium) solution of Eq. (2a) will have an error tending to zero as $\exp(-\sqrt{|\lambda_{\min}|}\, t)$. Here, $-\lambda_{\min}$ is the smallest eigenvalue (in absolute magnitude) of $f_\alpha$. For explicit time differencing of the force operator in Eq. (2a), the time step $\Delta t$ is limited by the numerical stability criterion $\Delta t \leq 2/\sqrt{|\lambda_{\max}|}$, where $-\lambda_{\max}$ is the largest eigenvalue of $f_\alpha$. Since $t = N\,\Delta t$, the number of iterations $N$ required for convergence to a fixed error scales as $N \sim \sqrt{\lambda_{\max}/\lambda_{\min}} \equiv P^{1/2} \simeq N_s$, where $N_s$ is the number of radial mesh points. For the refined radial meshes of interest for local mode analysis ($N_s \geq 10^2$), this scaling can be prohibitive.

One way to improve the convergence rate of Eq. (A2) is to reduce $P$. (Another possibility, not considered here, is to use a semi-implicit time-differencing scheme for the force operator.) This can be accomplished by multiplying (or conditioning) the force vector $\mathbf{F}$ (with $(\mathbf{F})_\alpha \equiv \mathbf{F}_\alpha^{mn}$) by a positive-definite matrix $\mathbf{M}$. ($\mathbf{M}$ must be positive definite so that the energy minimization property of Eqs. (2) is retained.) The preferred choice for $\mathbf{M}$ would be the negative inverse of the Hessian matrix of $W$; i.e., $\mathbf{M} = -(\partial^2 W/\partial \mathbf{X}\, \partial \mathbf{X})^{-1}$. With $\mathbf{M}$ chosen in this way, the eigenvalues of the "preconditioned" force, $\mathbf{F}_* \equiv \mathbf{M} \cdot \mathbf{F}$, would all be $-1$, and Eqs. (2) would theoretically converge in only a few iterations (independent of $N_s$). However, for MHD problems in three spatial dimensions, it is impractical to compute and invert the full Hessian matrix, which includes the Fourier mode number, as well as radial, couplings. (In matrix language, the discretization of $\mathbf{F}$ does not yield a sparse, or banded, matrix.)

A practical preconditioning matrix $\mathbf{M}$ for the MHD problem may be obtained as the inverse of an approximate linearized operator. This operator is derived by averaging the coefficients of the highest derivatives in the exact MHD force operator over the angles $\theta$ and $\phi$. The resulting linear second-order operator in real space, $\tilde{f}_\alpha$, has coefficients which are functions of the radial coordinate ($s$) alone and thus can be easily inverted in Fourier space. It is found numerically that the inverse $\tilde{f}_\alpha^{-1}$ is an accurate approximation to the inverse Hessian, and therefore it is also a suitable preconditioner.

Let the approximation to $f_\alpha$ be given by

$$\tilde{f}_\alpha = \frac{\partial}{\partial s} D_\alpha^{ss}(s) \frac{\partial}{\partial s} + D_\alpha^{\theta\theta}(s) \frac{\partial^2}{\partial \theta^2} + D_\alpha^{\phi\phi}(s) \frac{\partial^2}{\partial \phi^2}, \tag{3}$$

where the diffusion coefficients $D_\alpha^{ij} > 0$ are defined below. (Recall $f_{\alpha=1} \equiv f_R$ and $f_{\alpha=2} \equiv f_Z$.) In Fourier space, the preconditioned evolution equation which replaces Eq. (2a) becomes

$$L_t(X_\alpha^{mn}) = -[\tilde{F}_\alpha^{-1} F_\alpha(\mathbf{X})]^{mn} \equiv Y_\alpha^{mn}(\mathbf{X}). \tag{4}$$

Here, $Y_\alpha^{mn}$ is the Fourier component of the preconditioned force operator. It satisfies the equation

$$\tilde{F}_\alpha^{mn} Y_\alpha^{mn} = -F_\alpha^{mn}(\mathbf{X}), \tag{5a}$$

where $\tilde{F}_\alpha^{mn}$ is the Fourier-space representation of the operator $\tilde{f}_\alpha$ given in Eq. (3):

$$\tilde{F}_\alpha^{mn} = \frac{\partial}{\partial s} D_\alpha^{ss} \frac{\partial}{\partial s} - m^2 D_\alpha^{\theta\theta} - n^2 D_\alpha^{\phi\phi}. \tag{5b}$$

For fixed values of $m$ and $n$, the discretization of Eq. (5a) on a radial mesh yields

$$M_{ij}^{mn} \cdot Y_\alpha^{mn}(s_j) = F_\alpha^{mn}(s_i), \tag{6a}$$

where $\mathbf{M}^{mn}$ is a negative-definite tridiagonal matrix:

$$M_{ij}^{mn} = \begin{cases} \dfrac{D_\alpha^{ss}(s_{i-1/2})}{\Delta s^2}, & j = i-1, \\ -\dfrac{D_\alpha^{ss}(s_{i-1/2}) + D_\alpha^{ss}(s_{i+1/2})}{\Delta s^2} - m^2 D_\alpha^{\theta\theta}(s_i) - n^2 D_\alpha^{\phi\phi}(s_i), & j = i, \\ \dfrac{D_\alpha^{ss}(s_{i+1/2})}{\Delta s^2}, & j = i+1. \end{cases} \quad (6b)$$

The explicit preconditioning matrix given in Eq. (6b) is determined at the radial grid points $j=1$ and $j=N_s$ by boundary conditions at $s=0$ and $s=1$, respectively. At the magnetic axis $s=0$ ($j=1$), which is an interior point of the polar flux coordinates, regularity of the solution requires $D_\alpha^{ss}=0$. This provides a natural boundary condition for the $m=0$ modes. For modes with $m>0$, $X_\alpha^{mn}(0)=0$ implies that only the block $i>1$, $j>1$ needs to be retained in Eq. (6b). For plasma configurations with a prescribed (fixed) boundary at $s=1$ ($j=N_s$), $dX_\alpha^{mn}(1)/dt=0$. $M_{ij}^{mn}$ is therefore restricted to the block $i<N_s$, $j<N_s$. For free-boundary plasmas, the values of $X_\alpha^{mn}$ at $s=1$ are determined by the continuity of pressure. This case is treated by inserting a "ghost point" [8] one mesh point beyond $s=1$. The values of $X_\alpha^{mn}$ at this imaginary point are fixed, and this results in the truncation of $M_{ij}^{mn}$ for $j>N_s$, with $D_\alpha^{ss}(s_{i-1/2}) + D_\alpha^{ss}(s_{i+1/2}) \to 2D_\alpha^{ss}(s_{i-1/2})$ at $i=j=N_s$.

Explicit forms for the diffusion elements are easily derived from the MHD forces [5]. The result is

$$D_R^{ss} = 2\left\langle \frac{(Z_\theta R)^2 P_B}{\sqrt{g}} \right\rangle, \quad (7a)$$

$$D_R^{\theta\theta} = \left\langle \frac{R^2}{\sqrt{g}} \{ Z_s^2 [(B^\theta Z_\theta + B^\phi Z_\phi)^2 + (RB^\phi)^2] + (R_s Z_\theta B^\theta + R_\phi Z_s B^\phi)^2 \} \right\rangle, \quad (7b)$$

$$D_R^{\phi\phi} = \langle (B^\phi)^2 \sqrt{g} \rangle = D_Z^{\phi\phi}, \quad (7c)$$

$$D_Z^{ss} = 2\left\langle \frac{(R_\theta R)^2 P_B}{\sqrt{g}} \right\rangle, \quad (7d)$$

$$D_Z^{\theta\theta} = \left\langle \frac{R^2}{\sqrt{g}} \{ R_s^2 [(B^\theta R_\theta + B^\phi R_\phi)^2 + (RB^\phi)^2] + (R_\theta Z_s B^\theta + R_s Z_\phi B^\phi)^2 \} \right\rangle. \quad (7e)$$

Here, $P_B = B^2/2\mu_0$ is the magnetic pressure, $\langle A \rangle = (2\pi)^{-2} \iint A \, d\theta \, d\phi$ denotes a flux surface average, and the subscripts $s$, $\theta$, and $\phi$ on $R$ and $Z$ denote differentiation (e.g., $R_s \equiv \partial R/\partial s$). The metric elements are $g_{ij} = R_i R_j + Z_i Z_j + \delta_{i\phi}\delta_{j\phi} R^2$, $\sqrt{g} = \partial(R, Z)/\partial(s, \theta)$ is the Jacobian, and $B^i \equiv \mathbf{B} \cdot \nabla i$, for $i = \theta, \phi$, are the contravariant components of the magnetic field.

From the preconditioned evolution Eq. (4), it follows that the convergence rate

will now be determined by the condition number of the discrete approximation to $(\tilde{F}^{-1}F)^{mn}$. Since both $\tilde{F}^{mn}$ and $F^{mn}$ have condition numbers $P \sim (N_s^2 + c_1 m^2 + c_2 n^2)$ ($c_i$ are constants, and $m$ and $n$ are the poloidal and toroidal Fourier mode numbers, respectively), it follows that the condition number for the composite operator $(\tilde{F}^{-1}F)^{mn}$ is $O(1)$. As a result, the number of iterations required for convergence of the preconditioned equations should be independent of the mesh size. This conclusion, however, applies rigorously only to the linearized operator in the neighborhood of an equilibrium. Thus, there may still be some residual dependence on the mesh size for the full nonlinear problem.

## 3. Results

The impact of the preconditioning algorithm on the iteration defined in Eq. (A2) can be demonstrated by considering a pair of numerical examples. The first case is the determination of a fixed-boundary equilibrium for the Advanced Toroidal Facility

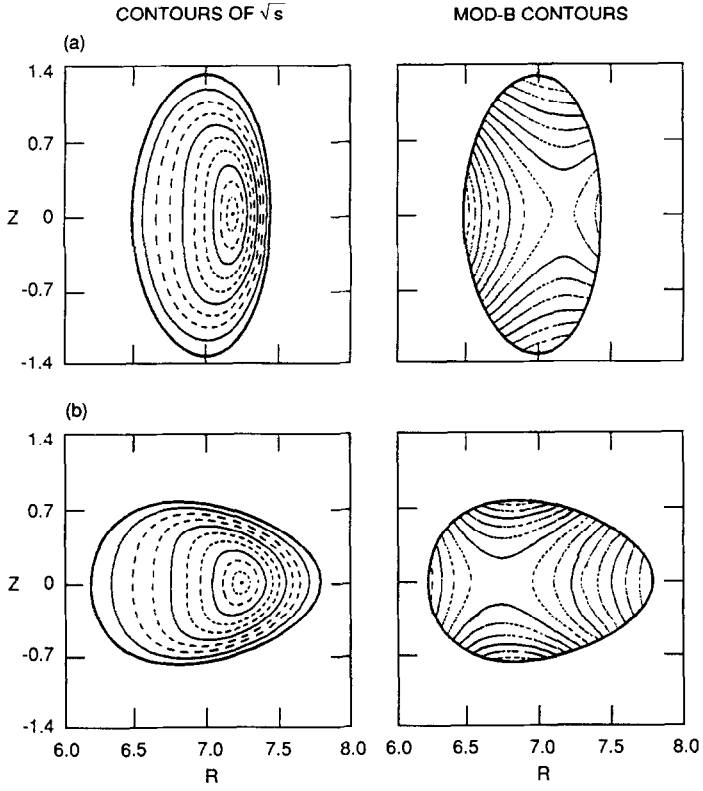


FIG. 1. Equilibrium magnetic flux surfaces and $|\mathbf{B}|$ contours for the ATF fixed boundary device at the two symmetry planes $N_F\phi = 0$ and $N_F\phi = \pi$ ($N_F = 12$): (a) $N_F\phi = 0$; (b) $N_F\phi = \pi$.

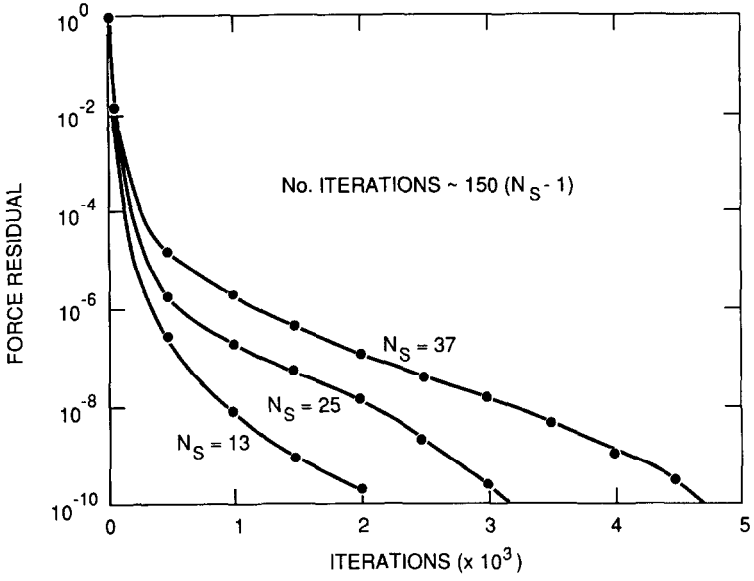


FIG. 2. Reduction of force residual, $|\mathbf{F}|^2$, vs iteration number for radial meshes $N_s = 13$, 25, and 37. No preconditioning was applied.

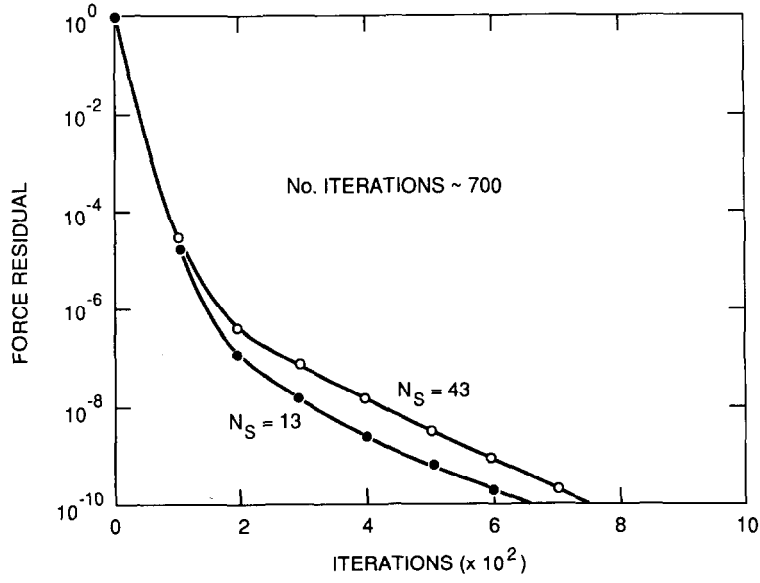


FIG. 3. Reduction of force residual, $|\mathbf{F}|^2$, vs iteration number for radial meshes $N_s = 13$ and 43. Preconditioning has been applied.

(ATF) [9]. ATF is an $l=2$, $N_F=12$ field period torsatron with a boundary surface approximated by

$$R = 6.88 + 0.86\cos\theta - 0.24\cos(\theta - N_F\phi) + 0.10\cos 2\theta - 0.03\cos(2\theta - N_F\phi), \quad (8a)$$

$$Z = \sin\theta + 0.24\sin(\theta - N_F\phi) - 0.02\sin 2\theta + 0.03\sin(2\theta - N_F\phi). \quad (8b)$$

The units used in Eqs. (8) render the mean minor radius nearly equal to one. The computations reported here correspond to a plasma pressure with $\langle\beta\rangle = 0.0125$ and $\beta_{\text{peak}} = 0.036$, where $\beta = 2\mu_0 p/B^2$. The rotational transform profile $i(s) \equiv \langle B^\theta\rangle/\langle B^\phi\rangle$ is computed from the requirement that the net toroidal current, $\langle \mathbf{J}\cdot\nabla\phi\rangle$, should vanish in steady state on each magnetic flux surface. Figure 1 shows the magnetic flux surfaces ($s=$ const surfaces) and $|\mathbf{B}|$ contours for a converged ATF equilibrium in the two symmetry planes $N_F\phi = 0$ and $N_F\phi = \pi$. The magnetic surfaces increase linearly with $\sqrt{s}$ from $s=0$ (the central magnetic axis point) to $s=1$ at the enclosing boundary curve. The convergence of the force residual, $|\mathbf{F}|^2$, for several radial grids is shown in Fig. 2 (computed without preconditioning) and Fig. 3 (computed with preconditioning). These computations

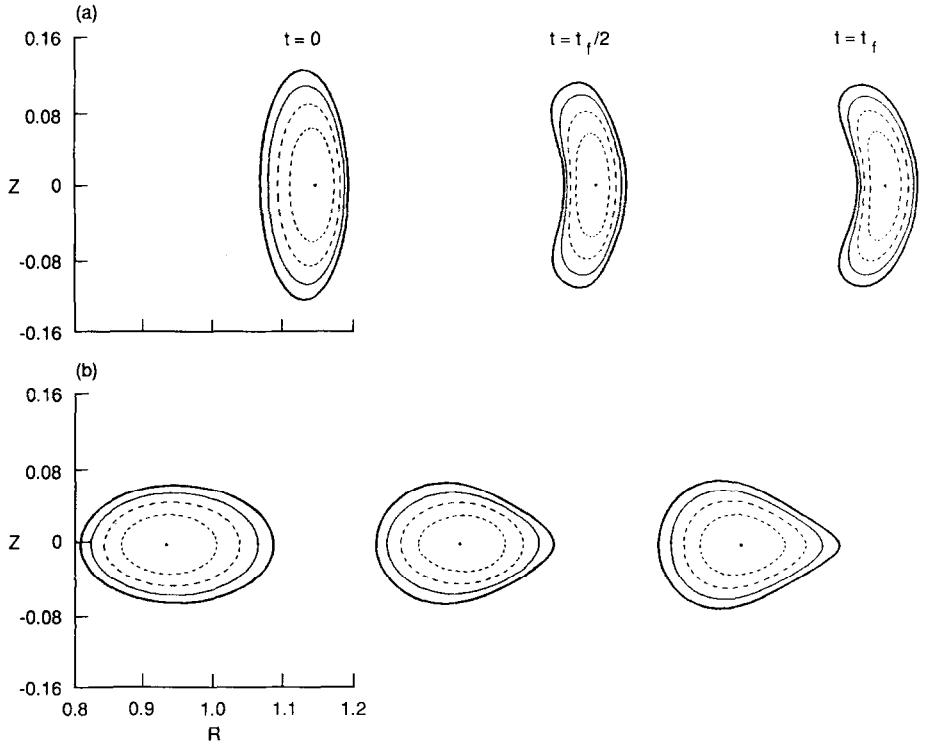


FIG. 4. Free-boundary magnetic flux surface evolution for the Helias configuration in the two symmetry planes $N_F\phi = 0$ and $N_F\phi = \pi$ ($N_F = 5$).

were performed with a poloidal mode number spectrum $m = 0, ..., 6$ and toroidal mode number spectrum $n = -3, ..., 3$ (in multiples of $N_F$) used in Eq. (1).

The unpreconditioned convergence sequence exhibits a nearly linear dependence for the number of iterations $I$ needed to attain a normalized force residual $|\mathbf{F}|^2 < 10^{-10}$: $I \sim 150(N_s - 1)$. In contrast, $I \lesssim 700$ is nearly independent of $N_s$ when the preconditioning algorithm is applied. Thus, for radial meshes with $N_s > 5$, there is a significant improvement in temporal convergence due to preconditioning. (The numerical overhead associated with computing the matrix elements of Eq. (6) and inverting the tridiagonal matrix $\mathbf{M}$ is negligible.) Note the difference in horizontal scales (representing the iteration number) in Figs. 2 and 3. For the finest grids shown, the preconditioned iteration converges nearly six times as fast as the original iteration. In fact, for $N_s > 43$, the original iteration may cease to converge below $|\mathbf{F}|^2 \sim 10^{-9}$. For $N_s = 100$, the preconditioned scheme converged to $|\mathbf{F}|^2 = 10^{-10}$ in 1400 iterations. This result suggests that there might be a remaining (though weak) dependence of $I$ on the radial grid size, $N_s$.

The next example is a computation for a free-boundary Helias [10] configuration. For this case, the outermost magnetic flux surface ($s = 1$) is allowed to deform until there is no jump in the magnetic pressure, $B^2/2\mu_0$, at this surface. Self-consistent flux surfaces are shown for Helias in Fig. 4 in the two symmetry planes $N_F\phi = 0$ and $N_F\phi = \pi$ ($N_F = 5$). The temporal evolution from the initial boundary configuration—chosen for simplicity to be a helically rotating ellipse—to the final (strongly deformed) equilibrium state was computed by using VMEC for the internal plasma force balance and NESTOR [11] to compute the vacuum field at the

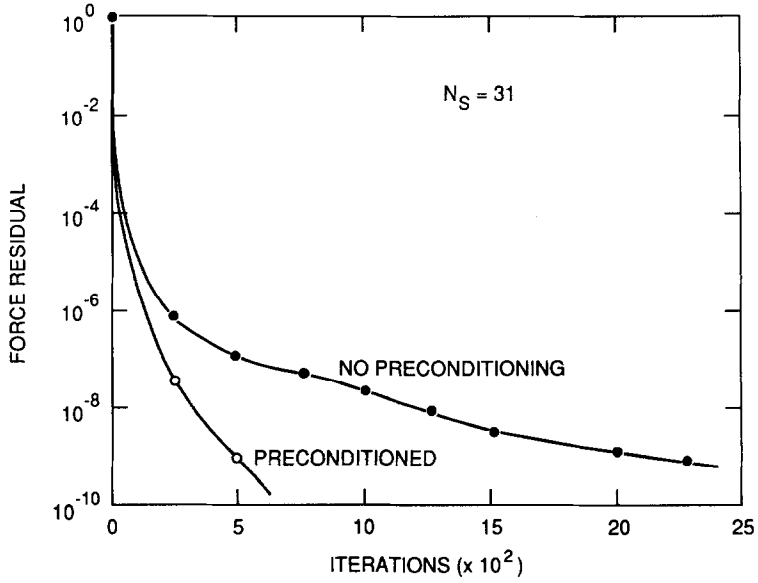


FIG. 5. Effect of preconditioning on the free-boundary evolution of Helias.

plasma–vacuum interface. For the plasma, modes with $m = 0, ..., 4$ and $n = -4, ..., 4$ were used. The vacuum field is the sum of the magnetic field arising from the external Helias coils alone (in the absence of plasma) plus the induced field required to satisfy $\mathbf{B} \cdot \mathbf{n} = 0$ at the last magnetic flux surface ($s = 1$). Here, $\mathbf{n}$ is the vector normal to the plasma surface at $s = 1$. In Fig. 5 the convergence rate is shown for this Helias computation with $N_s = 31$ radial grid points. Once again, the preconditioned iteration scheme shows a substantial reduction in the number of iterations required to attain a fixed level of force residual.

## 4. Conclusion

A preconditioning algorithm for the inverse MHD equilibrium equations has been derived. It is easily implemented and leads to a convergence rate that is essentially independent of the number of radial grid points, $N_s$. This represents a significant improvement over previous schemes that have convergence rates scaling linearly with $N_s^{-1}$.

## Appendix A

The relationship of the time evolution operator in Eq. (2a) to the method of conjugate gradients can be demonstrated by integrating Eq. (2a) from $t = t_n$ to $t = t_{n+1} \equiv t_n + \Delta t$. Assuming that $1/\tau$ and $\mathbf{F}$ vary slowly in this time interval yields (to lowest order in $\Delta t$):

$$\mathbf{V}_{n+1} \exp(t_{n+1}/\tau) = \mathbf{V}_n \exp(t_n/\tau) + \exp(t_{n+1}/\tau)\, \mathbf{F}(\mathbf{X}_n), \tag{A1}$$

where $\mathbf{V} \equiv d\mathbf{X}/dt$ and $\mathbf{F}(\mathbf{X}_n) \equiv \mathbf{F}[\mathbf{X}(t_n)]$. Introducing $\mathbf{P}_n \equiv \mathbf{V}_n/\Delta t$ and noting that the optimum damping rate is given by $1/\tau = -d(\ln |\mathbf{F}|^2)/dt$ (corresponding to critical damping of the longest spatial wavelength modes), Eq. (A1) becomes

$$\mathbf{P}_n = \beta_n \mathbf{P}_{n-1} + \mathbf{F}(\mathbf{X}_n). \tag{A2a}$$

The $\mathbf{X}_n$ iteration is simply

$$\mathbf{X}_{n+1} = \mathbf{X}_n + \alpha_n \mathbf{P}_n, \tag{A2b}$$

where $\alpha_n \equiv (\Delta t)^2$ and $\beta_n = |\mathbf{F}|_n^2 / |\mathbf{F}^2|_{n-1}$.

Since $-\mathbf{F}$ is the gradient of the energy functional $W$, Eq. (A2a) is the standard conjugate gradient choice for the search direction $P_n$. The main difference in the present iteration scheme is in the choice of the time-step parameter $\Delta t$ which determines $\alpha_n$ in Eq. (A2b). In the usual conjugate gradient method, the Hessian is computed to determine the step length ($\alpha_n$) required to minimize $W$ along the search direction. In our nonlinear problem, this method is too complicated and

time-consuming. Instead, $\Delta t$ is required to satisfy the Courant–Friedrichs–Levy stability condition for explicit time discretizations of hyperbolic partial differential equations.

## ACKNOWLEDGMENTS

The authors thank N. Dominguez, W. I. van Rij, and R. N. Morris for their careful reading of this manuscript and their helpful suggestions.

## REFERENCES

1. S. P. HIRSHMAN, U. SCHWENN, AND J. NÜHRENBERG, *J. Comput. Phys.* **87**, 396 (1989).
2. O. BETANCOURT, *Commun. Pure Appl. Math.* **41**, 551 (1988).
3. F. BAUER, O. BETANCOURT, AND P. GARABEDIAN, *Magnetohydrodynamic Equilibrium and Stability of Stellarators* (Springer-Verlag, New York, 1984).
4. P. E. GILL, W. MURRAY, AND M. H. WRIGHT, *Practical Optimization* (Academic Press, New York, 1981), p. 551.
5. S. P. HIRSHMAN AND J. C. WHITSON, *Phys. Fluids* **26**, 3553 (1983).
6. M. HESTENES, *Conjugate Direction Methods in Optimization* (Springer-Verlag, New York, 1980).
7. P. GARABEDIAN, *Partial Differential Equations* (Wiley, New York, 1964).
8. G. D. SMITH, *Numerical Solution of Partial Differential Equations: Finite Difference Methods* (Oxford University Press, Oxford, 1978).
9. J. F. LYON *et al.*, *Fusion Technol.* **10**, 179 (1986).
10. J. NÜHRENBERG AND R. ZILLE, paper presented at the 1988 Sherwood Theory Conference, Gatlinburg, Tennessee, April 18–20, 1988; P. MERKEL, in *Proceedings, 2nd Workshop on Wendelstein VII-X, Schloss Ringberg, 1988*, edited by F. Rau and C. G. Leotta (CEC, Brussels, 1988).
11. P. MERKEL, *J. Comput. Phys.* **66**, 83 (1986).